



UNIVERSITY OF LEEDS

This is a repository copy of *Drone Empowered Small Cellular Disaster Recovery Networks for Resilient Smart Cities*.

White Rose Research Online URL for this paper:

<http://eprints.whiterose.ac.uk/104809/>

Version: Accepted Version

Proceedings Paper:

Hayajneh, A, Zaidi, SAR, McLernon, DC et al. (1 more author) (2016) Drone Empowered Small Cellular Disaster Recovery Networks for Resilient Smart Cities. In: 2016 IEEE International Conference on Sensing, Communication and Networking (SECON Workshops). SECON 2016, 27-30 Jun 2016, London, UK. IEEE . ISBN 978-1-5090-2429-2

<https://doi.org/10.1109/SECONW.2016.7746806>

(c) 2016, IEEE. Personal use of this material is permitted. Permission from IEEE must be obtained for all other uses, in any current or future media, including reprinting/republishing this material for advertising or promotional purposes, creating new collective works, for resale or redistribution to servers or lists, or reuse of any copyrighted component of this work in other works.

Reuse

Unless indicated otherwise, fulltext items are protected by copyright with all rights reserved. The copyright exception in section 29 of the Copyright, Designs and Patents Act 1988 allows the making of a single copy solely for the purpose of non-commercial research or private study within the limits of fair dealing. The publisher or other rights-holder may allow further reproduction and re-use of this version - refer to the White Rose Research Online record for this item. Where records identify the publisher as the copyright holder, users can verify any specific terms of use on the publisher's website.

Takedown

If you consider content in White Rose Research Online to be in breach of UK law, please notify us by emailing eprints@whiterose.ac.uk including the URL of the record and the reason for the withdrawal request.

Drone Empowered Small Cellular Disaster Recovery Networks for Resilient Smart Cities

Ali Mohammad Hayajneh, Syed Ali Raza Zaidi, Des C. McLernon and Mounir Ghogho

Abstract—Resilient communication networks, which can continue operations even after a calamity, will be a central feature of future smart cities. Recent proliferation of drones propelled by the availability of cheap commodity hardware presents a new avenue for provisioning such networks. In particular, with the advent of Google's Sky Bender and Facebook's internet drone, drone empowered small cellular networks (DSCNs) are no longer fantasy. DSCNs are attractive solution for public safety networks because of swift deployment capability and intrinsic network reconfigurability. While DSCNs have received some attention in the recent past, the design space of such networks has not been extensively traversed. In particular, co-existence of such networks with an operational ground cellular network in a post-disaster situation has not been investigated. Moreover, design parameters such as optimal altitude and number of drone base stations, etc., as a function of destroyed base stations, propagation conditions, etc., have not been explored. In order to address these design issues, we present a comprehensive statistical framework which is developed from stochastic geometric perspective. We then employ the developed framework to investigate the impact of several parametric variations on the performance of the DSCNs. Without loss of any generality, in this article, the performance metric employed is coverage probability of a down-link mobile user. It is demonstrated that by intelligently selecting the number of drones and their corresponding altitudes, ground users coverage can be significantly enhanced. This is attained without incurring significant performance penalty to the mobile users which continue to be served from operating ground infrastructure.

Index Terms—Drone, Public safety, Stochastic geometry, Unmanned aerial vehicles, Coverage probability, Optimization, Heterogeneous networks.

I. INTRODUCTION

A. Motivation

In order to address increased demand for any-time/any-where wireless connectivity, both academic and industrial researchers are actively engaged in the design of fifth generation (5G) wireless communication networks. In contrast to traditional (i.e., bottom-up or horizontal) design approach, 5G wireless networks are being co-created with various stakeholders to address connectivity requirements across various verticals (i.e., employing a top-to-bottom approach). Most of these verticals belong to the grand vision of smart connected cities empowered via ubiquitous on-demand connectivity. One of the key features of smart connected cities is resilience by design. From communication networks perspective, this requires obliviousness under various failures. In the context of cellular networks, base station failures can be caused either due to natural or synthetic phenomenon. Natural phenomenon such as earth-quake or flooding can result in either destruction of communication hardware or disruption of energy supply to base stations. Man made destruction can be either due to a certain sub-system failure or alternatively due to vandalism. In such cases there is a dire need for a mechanism through which capacity short-fall can be met in a rapid manner. Drone empowered small cellular networks (DSCNs) or so-called flying cellular networks present an attractive solution as they can be swiftly deployed for provisioning public safety networks. The ability to self-organize either

This work is partially funded by The Hashemite University (HU), Zarqa, Jordan.

A. M. Hayajneh, S. A. R. Zaidi, Des. C. McLernon, and M. Ghogho are with the School of Electronic and Electrical Engineering, University of Leeds, Leeds LS2 9JT, United Kingdom, e-mail: elamh.s.a.zaidi,d.c.mclernon,m.ghogho@leeds.ac.uk. M. Ghogho is also affiliated with the International University of Rabat, Morocco.

in stand-alone or via remote configuration in an on-demand manner makes the flying cellular network a key enabler for resilient communication networks. Despite several recent efforts [1]–[4], the design and deployment of flying cells as a recovery network is not extensively investigated in the literature. So, in this paper, by borrowing the well-known tools from stochastic geometry, we will investigate the design space of flying cellular networks. We will also explore co-existence properties of an overlaid DSCN with the operational part of the existing network.

B. Related Work

In the recent past, public safety networking has received significant attention within the third generation partnership project (3GPP) standardization. 3GPP is currently in process of standardizing proximity services (ProSe) via Device-to-Device (D2D) communication. The central idea behind ProSe is to form an ad-hoc network where certain nodes of the network may still have access to operational cellular infrastructure in a post-disaster situation. These nodes can act as gateways for forwarding critical information to first responders. While D2D communication is a promising solution for public safety networks, there are several design challenges which need to be addressed to realize practical deployment. In particular, in multi-hop D2D communication networks, those nodes which are connected to cellular network may become traffic-forwarding hot-spots. Due to limited battery capacity of mobile user equipment, traffic hot-spots may reduce the operational lifetime of entire network. Moreover, the network in its essence is ad-hoc and thus guaranteeing reliable connectivity is not possible. In contrast, DSCNs present an attractive alternative and complementary deployment option. Since DSCNs are mostly operator deployed both: (i) interoperability amongst DSCNs nodes; and (ii) compatibility with operational cellular infrastructure can be ensured. Moreover, propagation conditions are much more favorable and can be further optimized by exploiting controlled mobility of UAVs. Consequently, it is envisioned that both D2D and DSCNs will complement the legacy private/professional mobile radio (PMR) (e.g., trans-European trunked radio (TETRA) and project 25 (P25)) for enabling next generation public safety networks [5]–[7]. In the recent past [1]–[4] numerous studies have attempted to define the design space of the DSCNs from various different perspectives. Nevertheless, most of them either: (i) study a simple single-cell set up; (ii) do not account for intrinsic randomness in topology; (iii) abstract the coverage areas and interference via non-realistic models. The authors in [4] investigated drone small cells (DSCs) deployment to provision air-to-ground services. The authors consider a device-centric deployment approach and adopt modeling abstraction of circular discs for the coverage areas induced by DSCs. Moreover, they investigate the optimal DSC altitude which leads to a maximum ground coverage and minimum required transmit power for a single DSC. Optimization for both: (i) distance between co-channel drones (i.e., drones sharing the same frequency) and (ii) the altitudes of co-channel drones was also performed. The study does not explore cross-tier interference management in the presence of large scale DSCN deployment. The authors in [8], based on the results of [9], present a 3D optimization problem for DSCs with the aim to maximize the number of users to be covered by such DSCs using a numerical search algorithm to satisfy the defined quality of service (QoS) measures. The paper focuses

on drone empowered future cellular networks for disaster recovery/public safety. Nevertheless, the effect of cross network interference (i.e., interference between operational cellular infrastructure and DSCs in a post-disaster scenario) has not been addressed. To this end, we now present a holistic framework for characterizing the performance of an overlaid DSCN which is collocated with operational cellular infrastructure. We explicitly investigate the co-existence properties of both networks in the presence of cross-network interference. Moreover, we also demonstrate that the desired performance metric can be significantly enhanced via optimal control of drone altitude. The optimal altitude for a large DSCN formed by more than two drone base stations (DBSs) is investigated for the first time.

C. Contributions

The contribution and organization of this paper are as follows:

- 1) The comprehensive spatial modeling of a drone-based public safety network is considered over a partially destructed/offloaded cellular network. The impact of various parameters such as path-loss, number of DBSs, density of micro base stations (MBSs) and the altitude of the DBSs on both the DSCN and the cellular network coverage has been investigated (see section II).
- 2) Borrowing tools from stochastic geometry, we present a statistical framework for quantifying the performance of large scale DSCNs deployment. The analytical framework is subsequently employed for design optimization.
- 3) The impact of the number of DBSs (and their height) on the coverage probability performance metric for both drone mobile users (DMUs) and micro mobile users (MMUs) (see section III).
- 4) Finally, some critical design issues are explored and envisioned future developments are summarized (see section V).

D. Notation.

Throughout this paper, we employ the following mathematical notations. The counting measure of a point process $\Phi(\mathcal{B})$ provides a count of points inside the compact closed subset (i.e., bounded area) $\mathcal{B} \in \mathbb{R}^2$. The probability density function (PDF) for a random variable X is represented as $f_X(x)$ with the cumulative density function as $F_X(x)$. The exclusion symbol \setminus to represent the exclusion of a subset from a superset. The expectation of a function $g(X)$ of a random variable X is represented as $\mathbb{E}_X[g(x)]$. The symbol W is used to represent the set of the entire space contained in the d -dimensional space \mathbb{R}^d . The ceiling of any number is represented by $\lceil \cdot \rceil$.

II. NETWORK AND PROPAGATION MODEL

A. Deployment Geometry

Consider the down-link communication in a network formed by a DSCN overlaid on an existing cellular network. As illustrated in Fig. 1, the disaster recovery network is established via deployment of a finite number of DBSs. The key objective is to complement the capacity of the operational cellular micro base stations serving the traffic originating from coverage hole created due to the destruction of infrastructure. The number of drones required to meet the shortfall in coverage is strongly coupled with: (i) the probability (p^o) of destruction of an arbitrary MBS; and (ii) the radius R_r of the affected area (i.e., the disaster recovery area). As shown in Fig. 1, it is assumed that in a post-disaster scenario some of the MBSs are destroyed (illustrated as the red framed points). Consequently, N_d drones are deployed to cover the destroyed cells. However, the number of drones is not necessarily the same as the number of the destroyed cells. This is due to the limitation on the capacity of the DBSs as well as the difference in transmission power and radio prorogation conditions when compared to the MBSs. For the modeling of the spatial distribution of the overall wireless network, we borrow tools

from stochastic geometry. To this end, it is assumed that N_d number of drones are uniformly distributed inside the two dimensional disc formed by the disaster recovery area. The overall network geometry is modeled with two collocated point process, the former for the operational MBSs while the later for the DBCN BSs, as follows:

- 1) **An inhomogeneous Poisson point process (IHPPP):** Here we define the inhomogeneous Poisson point process, $\Phi_m = \{x_1, x_2, \dots, x_N\} \subset \mathbb{R}^d$, as the superposition of two disjoint conditional PPPs: (i) a conditional PPP of density λ_1 such that $\Phi_1 = \{x_1, x_2, \dots, x_N \in W \setminus \mathcal{B}(0, R_r)^1\} \subset \mathbb{R}^d$ and (ii) a conditional PPP of points density λ_2 such that $\Phi_2 = \{x_1, x_2, \dots, x_N \in \mathcal{B}(0, R_r)\} \subset \mathbb{R}^d$. Hence, the probability of finding $n = n_1 + n_2$ points (i.e. n_1 points from Φ_1 and n_2 points from Φ_2) inside disc of radius $R > R_r$ can be obtained as

$$\mathbb{P}(\Phi_m(\mathcal{B}(0, R)) = n = n_1 + n_2) = \prod_{i=1}^2 \frac{(\lambda_i v(\mathcal{A}_i))^n}{n_i!} \exp(-\lambda_i v(\mathcal{A}_i)). \quad (1)$$

- where λ_i is the density of the base stations per unit area of \mathcal{A}_i (i.e., density of MBSs), $v(\mathcal{A}) = \int_{\mathcal{A}} dx$ is the Lebesgue measure [10]. In-particular, if the desired area is a ring with radii $A \leq r \leq B$, then $v(\mathcal{A}) = \pi(B^2 - A^2)$.
- 2) **Binomial point process (BPP):** While the IHPPP formulation is adequate to model operational cellular network MBSs, the above equation cannot be employed for the DSCN formed inside the recovery area $\mathcal{B}(0, R_r)$. That is because that the specific number of drones N_d when uniformly distributed in this finite area, $\mathcal{B}(0, R_r)$, form a binomial point process (BPP)² [11]. In particular, for a finite area of radius R_r in the N -dimensional space, the probability of having k transmitting interferers (i.e., co-channel drones) at the origin (i.e., the interference at $\mathcal{B}(0, 0)$) from the ring-shaped area $\mathcal{B}(0 \leq A < B \leq R_r)$ with, respectively, an inner and outer radius A and B inside $\mathcal{B}(0, R_r)$ can be evaluated as follows

$$\mathbb{P}(\Phi(\mathcal{B}(0 \leq A < B \leq R_r)) = k) = \binom{N_d}{k} \left(\frac{B^N - A^N}{R_r^N} \right)^k \left(1 - \frac{B^N - A^N}{R_r^N} \right)^{N_d - k}. \quad (2)$$

In summary, the spatial distribution of DSCs is captured using a BPP, while co-existing cellular network is modeled via thinned IHPPP as described above.

B. Propagation Model

- 1) **Path Loss Model:** In order to accurately capture the propagation conditions in a DSCN, we employ the path loss model presented in [4] which is derived from practical measurements. The employed path loss model adequately captures line of sight (LoS) and non line of sight (NLoS) contributions for drone-to-ground communication as follows:

$$l_{LoS}(h, r) = \frac{(r^2 + h^2)^{-1}}{K_{LoS}}, \quad (3)$$

$$l_{NLoS}(h, r) = \frac{(r^2 + h^2)^{-1}}{K_{NLoS}}, \quad (4)$$

where K_{LoS} and K_{NLoS} are environment and frequency dependent parameters such that $K_i = \zeta_i (c/(4\pi f_{MHz}))^{-\alpha}$, ζ_i is the excess

¹ $\mathcal{B}(0, R_r)$ denotes a ball of radius R_r centred at origin.

²The spatial distribution of the drones is their projection onto the two-dimensional coverage region. This, can be obtained by angular transformation of the geographical three-dimensional distribution of the DBCN.

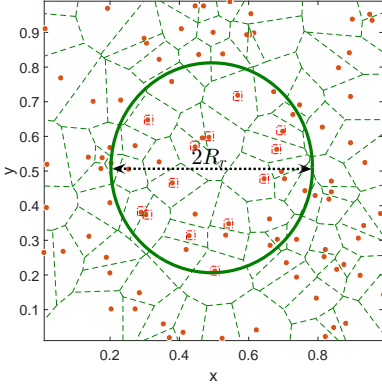


Fig. 1: One realization of the proposed network model. The green circle represents the recovery area of a radius R_r to be covered by drones (on the top of the existing cellular network). The small red points represent the MBSs. The red points (framed by a red square) represent the destroyed BSs (any BS inside the circle destroyed with probability $p^o = 0.5$).

path loss for $i \in \{LoS, NLoS\}$ and α is the path loss exponent which is equal to 2 as can be found in the literature of drone-based small cell applications. This propagation model categorizes the path loss exponent or the excess path loss into two groups depending on the probability of being in line of sight or not, whereas the majority on the literature categorizes into dual slope with regards to a threshold distance at which the slope of path loss curve switches to a different value. Furthermore, the probability of having a LoS link from the DSC and the desired mobile user (MU) is as follows:

$$\mathcal{P}_{LoS}(\theta) = \frac{1}{1 + a_1 e^{-b_1 \eta \theta + b_1 a_1}}, \quad (5a)$$

$$\mathcal{P}_{NLoS}(\theta) = 1 - \mathcal{P}_{LoS}(\theta), \quad (5b)$$

where a_1 , b_1 and c_1 are environment dependent constants, $\eta = 180/\pi$. Consequently, the total average excess path loss can be characterized as

$$\bar{\kappa}(r) = K_{LoS} + \frac{K_\Delta}{1 + a_1 e^{-b_1 \eta \tan^{-1}(\frac{h}{r}) + b_1 a_1}}. \quad (6)$$

where $K_\Delta = K_{LoS} - K_{NLoS}$, and $r = h/\tan(\theta)$. Note that, the average path loss from the DBS to the desired MU can be quantified from the above equations as

$$\bar{l}_d(r) = \frac{(r^2 + h^2)^{-1}}{\bar{\kappa}(r)}. \quad (7)$$

The large scale path loss for the down-link of the cellular network is modeled by the well-known power law path loss function

$$l_m(r) = \frac{r^{-\alpha}}{K}. \quad (8)$$

where α , the path loss exponent has typical values for small/micro cells between 2 and 4. K is the excess path loss and has typical values between 100 dB and 150 dB (see [12], [13] for details). The power law path loss is widely adopted in literature for analysis of large scale cellular networks³.

³An alternative general formula for the path loss is $l(r) = \frac{1}{K(\epsilon+r^\alpha)}$. This formula is widely used to mitigate the singularity at $r = 0$ and the divergence of the Laplace functional of aggregate interference with path loss exponent equal to or less than $\alpha \leq 2$. Here, ϵ is defined as the minimum distance between the transmitter and the receiver. This is implicitly incorporated for drone-based communication with $\epsilon = h^2$ [14].

C. Small scale Fading

It is assumed that large scale path loss is complemented with small scale Rayleigh fading such that $|g|^2 \sim \text{Exp}(1)$. Also, it is assumed that the network is operating in an interference limited regime, i.e., performance of all links is dependent upon co-channel interference and thermal noise at the receiver front-end is negligible.

III. COVERAGE PROBABILITY

In order to characterize the link level performance of DSCN, we employ coverage probability as a metric. The coverage probability of an arbitrary user is defined as the probability at which the received signal to interference ratio (SIR) is larger than a pre-defined threshold, β .

A. Coverage Probability of a stand-alone DSCN

In order to perform comparative analysis, we first quantify the performance of a stand-alone DSCN, (i.e., in absence of any cellular network). Without any loss of generality, we focus on the MU located at the center of the disaster recovery area as it is the most distant MU from the any MBS (i.e., worst MU with regards to average received power) and has the worst interference conditions (i.e., largest aggregate interference power) [15]. We also assume that N_c channels are assigned to the N_d DBSs to serve the traffic originating from the disaster recovery area. The received SIR at the DMU can be quantified as

$$SIR^{(d)} = \frac{|g|^2 P_d \bar{l}_d(r)}{I_{\Phi_d}^d}. \quad (9)$$

where P_d is the transmit power employed by the DBS and $I_{\Phi_d}^d$ is the aggregate interference from the co-channel transmitting DBSs experienced by the MU and can be written as $I_{\Phi_d}^d = \sum_{i \in \Phi_d \setminus \{0\}} |g_i|^2 P_d \bar{l}_d(r_i)$, where Φ_d is the set of all co-channel active DBSs. Consequently, the coverage probability for a DMU is given as

$$\begin{aligned} P_c^{(d)} &= \Pr\{SIR^{(d)} > \beta\}, \\ &= \mathbb{E}_r \left[\mathbb{E}_{I_{\Phi_d}^d} \left[\exp \left(-\frac{I_{\Phi_d}^d \beta}{P_d (r^2 + h^2)^{-1}} \right) \right] \right], \\ &= \mathbb{E}_r \left[\mathcal{L}_{I_{\Phi_d}^d}(s_1) \right] \end{aligned} \quad (10)$$

where $s_1 = \beta \bar{\kappa}(r) / (P_d (r^2 + h^2)^{-1})$, $\mathcal{L}_{I_{\Phi_d}^d}(s_1)$ is the Laplace transform of the aggregate interference and this can be evaluated as in (11), where N_c is the number of channels available and $\left[\frac{N_d}{N_c} \right]$ is to assure that the total number of the remaining co-working nodes is an integer number [11].

B. Coverage Analysis of co-existing DSCN and Cellular Network

We now characterize the coverage probability of the DSCN operating in presence of a partially destroyed ground cellular network. As highlighted before, we assume that ground BSs are destroyed with a certain probability p^o within a circular disaster-affected area. In practice, the shape of the disaster recovery area can be arbitrary and the probability of destruction can be function of a natural phenomenon. Also, destruction across various ground BSs will be correlated which can be catered for by redefining p^o . However, for the sake of generality and tractability we employ a baseline model where p^o is a uniform random variable independent from BS location. The post-disaster operational cellular network forms a IHPPP such that

$$\lambda(r) = \lambda_2 \mathbb{1}(r \leq R_r) + \lambda_1 \mathbb{1}(r > R_r) \quad (12)$$

$$\mathcal{L}_{I_{\Phi_d}^d}(s) = \left(1 - \frac{1}{R_r^2} \int_0^{R_r} \mathbb{E}_g \left[\left(1 - \exp \left(-\frac{s|g|^2 P_d}{(h^2 + t^2)\bar{\kappa}(t)} \right) \right) 2t \right] dt \right)^{\left[\frac{N_d}{N_c} \right] - 1} = \left(1 - \int_0^{R_r} \frac{2tsP_d}{R_r^2 (\bar{\kappa}(t)h^2 + \bar{\kappa}(t)t^2 + sP_m)} dt \right)^{\left[\frac{N_d}{N_c} \right] - 1}. \quad (11)$$

where λ_1 and λ_2 are respectively the original and the retained PPP density of the cellular network before and after destruction. Here, we will quantify the overall coverage by studying: (i) the coverage probability for the DMU and (ii) the coverage probability for a MMU. To this end, the SIRs at the DMU and MMU can be respectively quantified as

$$SIR^{(d)} = \frac{|h_o|^2 P_d \bar{l}_d(r)}{I_{tot}^{(d)}}, \quad SIR^{(m)} = \frac{|h_o|^2 P_m l_m(r)}{I_{tot}^{(m)}} \quad (13)$$

where P_d and P_m are the transmitted signal power from the DBS and MBS, respectively, $I_{tot}^{(d)} = I_{\Phi_d}^d + I_{\Phi_m}^d$ and $I_{tot}^{(m)} = I_{\Phi_d}^m + I_{\Phi_m}^m$ are, respectively, the total aggregated co-channel interference seen by any down-link user located at the origin of the coverage area, and can be written as $I_{\Phi_d}^d = \sum_{i \in \Phi_d \setminus \{0\}} |g_i|^2 P_d \bar{l}_d(r_i)$, $I_{\Phi_m}^d = \sum_{i \in \Phi_m} |g_i|^2 P_m l_m(r_i)$, $I_{\Phi_m}^m = \sum_{i \in \Phi_m \setminus \{0\}} |g_i|^2 P_d \bar{l}_d(r_i)$ and $I_{\Phi_d}^m = \sum_{i \in \Phi_d} |g_i|^2 P_m l_m(r_i)$. Thus, the coverage probability, $P_c^{(d)}$, for any DMU in the coverage of a DBS can be written in the same way as in (10) as follows:

$$P_c^{(d)} = \Pr\{SIR^{(d)} > \beta\}, \\ = \mathbb{E}_r \left[\mathcal{L}_{I_{\Phi_d}^d}(s_1) \mathcal{L}_{I_{\Phi_m}^m}(s_2) \right]. \quad (14)$$

Note here, that the Laplace transform of the total interference can be evaluated by simply applying the convolution property of Laplace transforms as $\mathcal{L}_{I_{tot}^{(d)}}(s) = \mathcal{L}_{I_{\Phi_d}^d}(s) \mathcal{L}_{I_{\Phi_m}^m}(s)$. Next, the coverage probability at the MMU can be evaluated in the same way as in (10) and (14) as

$$P_c^{(m)} = \Pr\{SIR^{(m)} > \beta\}, \\ = \mathbb{E}_r \left[\mathcal{L}_{I_{\Phi_m}^m}(s_2) \mathcal{L}_{I_{\Phi_d}^d}(s_1) \right]. \quad (15)$$

where $s_2 = K\beta/(P_m r^{-\alpha})$. In order to evaluate the Laplace transform of the aggregate interference for the MMUs, we can write the following:

$$\mathcal{L}_{I_{\Phi_m}^m}(s) = \mathbb{E}(\exp(-sI_{\Phi_m})), \\ = \mathbb{E} \left(\prod_{x_i \in \Phi_m} \mathbb{E}_G \left(\exp(-s|g|^2 l_m(r)) \right) \right) \quad (16)$$

which can be solved using the generating functional of PPP as in [16], [17] such that

$$\mathcal{L}_{I_{\Phi_m}^m}(s) = \exp \left(- \underbrace{\int_0^\infty \left(1 - \mathbb{E}_G \left(-sP_m K |g|^2 l_m(r) \right) \right) \lambda(r) 2\pi r dr}_{A_1} \right). \quad (17)$$

Here, using the nodes density in (12), then A_1 in (17) can be written as

$$A_1 = \frac{2\pi \lambda_2 R_r^2}{\alpha} {}_2F_1 \left(1, \frac{2}{\alpha}; \frac{\alpha+2}{\alpha}; -\frac{R_r^\alpha}{sKP_m} \right) \\ + \frac{2sKP_m \pi \lambda_1 R_r^{2-\alpha}}{\alpha-2} {}_2F_1 \left(1, \frac{\alpha-2}{\alpha}; 2 \frac{\alpha-1}{\alpha}; -sKP_m R_r^{-\alpha} \right).$$

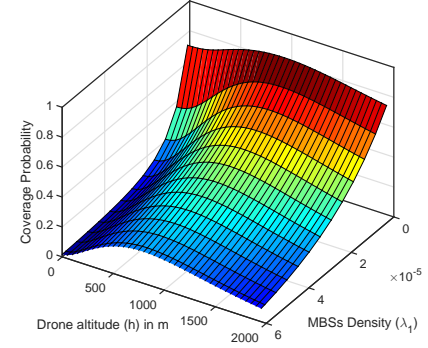


Fig. 2: Coverage probability for a drone mobile user at the center of the recovery area with both the DBSs and the MBSs sharing interference. The total available channels is 3. The destruction probability inside the recovery area is $p^o = 0.5$, with $\alpha = 4$, $R_r = 2$ km, $N_d = 6$, and $\beta = -3$ dB (see (14)).

where ${}_2F_1(a, b; c; d)$ is the Gauss Hyper-geometric function. One can solve this equation by change of variables, change of integral boundaries and finally using the identity $\int_0^u x^{\mu-1}/(1+\beta x)^v = \frac{u^\mu}{\mu} {}_2F_1(\mu, v; 1+\mu; -\beta u)$ as in Eq.3.194.1-3 [18].

C. Link Distance Analysis

The coverage probability derived in the previous sub-section for the MU is strongly dependent upon link distance. Consequently, $P_c^{(m)}$ and $P_d^{(m)}$ are conditional coverage probabilities as a function of user association model. In this article, we assume that the user associates to the nearest base station. Consequently, the conditional coverage probability derived in the previous sub-section must be averaged over the random link distance. To this end, in this sub-section we characterize the distribution of the link distance: (i) between DBS and its corresponding DMU and (ii) the MBS and its down-link MMU.

1) *Distance between DMU and DBS:* Since DBSs are uniformly distributed in the disaster area, the distance between a DMU at the origin and the DBS can be quantified from the void probability of a BPP as follows [19]:

$$f_R(r) = \frac{2N_d}{r} \left(1 - \left(\frac{r}{R_r} \right)^2 \right)^{N_d-1} \left(\frac{r}{R_r} \right)^2. \quad (18)$$

2) *Distance between MMU and serving MBS:* From a stochastic geometry analysis for homogeneous PPP with a density λ , it is well known that the distance PDF of the nearest node can be written as $f_R(r) = 2\pi r \lambda e^{-\pi r^2 \lambda}$ [10]. Hence, the cumulative density function (CDF) for the nearest neighbor can be written as $F_R(r) = 1 - e^{-\pi r^2 \lambda}$. In case of the post-disaster operational cellular network, the PPP assumption does not hold. As highlighted before, the MBSs form an IHPPP for which the link distance distribution has not been explored in the existing literature. Consequently, in the following proposition, we present an expression for the PDF of the distance between the MBS and its corresponding MMU.

TABLE I: Simulation parameters.

Parameter	Value	Description
$\zeta_{LoS}, \zeta_{NLoS}$	1,20 dB	Excess path loss
f_{MHz}	1800 MHz	Carrier frequency
α	4	Path loss exponent
K	132 dB	Excess path loss for micro cells
a_1, b_1	9.6, 0.28	Environment dependent constants
λ_1	1×10^{-5}	Base stations density
N_c	3	Available number of channels
P_d	1 dBW	Drone cell transmission power
P_m	10 dBW	Small BS cell transmission power

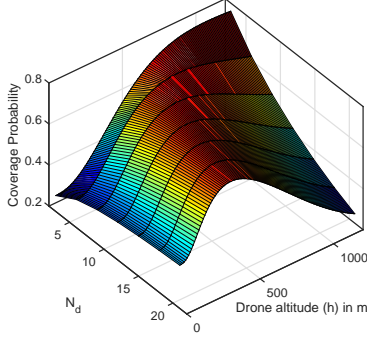


Fig. 3: Coverage probability at the center of the recovery area for drone mobile user with both the DBSs and the MBSs sharing interference. The total available channels is 3. The destruction probability inside the recovery area is $p^o = 0.5$. The MBS density of the original network $\lambda_1 = 1 \times 10^{-5}$, with $\alpha = 4$, $R_r = 3$ km and $\beta = -3$ dB (see (14)).

Proposition 1. *The PDF of the distance between the MMU at the center of the recovery area and the nearest MBS can be written as follows:*

$$f_R(r) = \exp(-\pi\lambda_2 R_r^2)(2\pi\lambda_1 r \exp(-\pi\lambda_1(r^2 - R_r^2))) + (1 - \exp(-\pi\lambda_2 R_r^2))(2\pi\lambda_2 r e^{-\pi r^2 \lambda_2}). \quad (19)$$

Proof. We assume that the resulting IHPPP is the superposition of two conditioned PPPs (i.e., the first with nodes density λ_2 (with any node $x_{\{2,i\}} \in \mathcal{B}(0, R_r)$) and the second with density λ_1 (with any node $x_{\{1,i\}} \in W \setminus \mathcal{B}(0, R_r)$)). Furthermore, the MMU is only connected to a MBS outside the recovery area, if and only if, there are no operational BSs inside the recovery area. In other words, this is when the recovery area acts as a hole with radius R_r . Thus, the probability that the distance to the nearest neighbor MBS, R , is greater than R_r can be quantified as follows:

$$\begin{aligned} F_R^{(1)}(r) &= 1 - \Pr(R \geq r), \\ &= 1 - \Pr(\text{Number of points of } \Phi_1 \\ &\quad \text{inside the set } \{\mathcal{B}(0, r) \setminus \mathcal{B}(0, R_r)\} = 0), \\ &= 1 - \exp(-\pi\lambda_1(r^2 - R_r^2)). \end{aligned} \quad (20)$$

Next, by differentiating the expression in (20) the PDF can be obtained as

$$f_R^{(1)}(r) = 2\pi\lambda_1 r \exp(-\pi\lambda_1(r^2 - R_r^2)). \quad (21)$$

Then, we average the nearest neighbor CDFs of the hypothetical Φ_1 and Φ_2 over the void probability of Φ_2 to obtain the average CDF of the nearest neighbor distance to the MMU as

$$\begin{aligned} F_R(r) &= v_2^o F_R^{(1)}(r) + (1 - v_2^o) F_R^{(2)}(r), \\ &= \exp(-\pi\lambda_2 R_r^2)(1 - \exp(-\pi\lambda_1(r^2 - R_r^2))) \\ &\quad + (1 - \exp(-\pi\lambda_2 R_r^2))(1 - e^{-\pi r^2 \lambda_2}) \end{aligned} \quad (22)$$

where v_2^o is the void probability of the PPP with density λ_2 which models the nodes inside the recovery area. Thus by simply differentiating $F_R(r)$ in (22) we can write (19) \square

IV. RESULTS AND DISCUSSION

In this section, we show numerical results for the coverage probabilities (P_c^d) and (P_c^m) of drone-based communication recovery network deployment. Furthermore, we assume that the DBCN is operating in

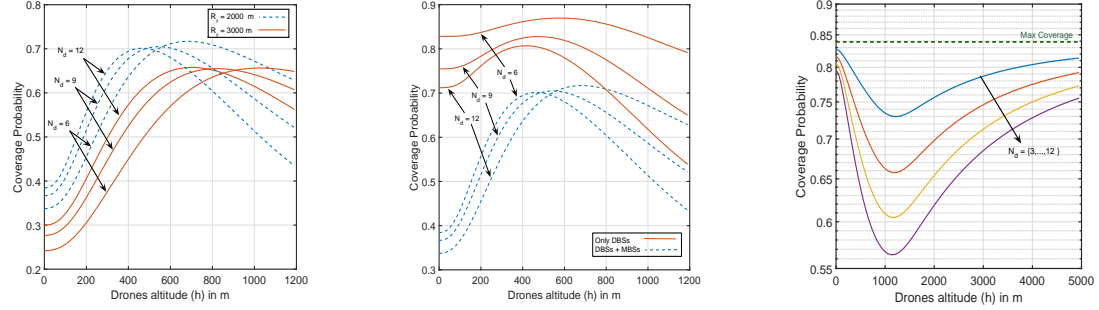
an urban environment with the parameters shown in Table I. Also, as described in the previous sections, we consider a Rayleigh fading wireless channel.

Fig. 2 shows the coverage probability for a DMU that is located at the center of the recovery area (see (14)). The coverage probability is plotted against both the MBSs density (λ_1) and the DBSs altitude (h). An interesting observation here is that the drone-based recovery network can achieve a significant enhancement of the coverage probability when the MBS density is around a certain value. For example, with an MBS density equal to $\lambda_1 = 1 \times 10^{-5}$, a minimum coverage probability $P_c^{(d)} = 0.8$ can be obtained. That is, the deployment of drones as a recovery network can be utilized to the maximum for small/micro cells (i.e., with average micro cell radii between $200 < R_{avg} < 1000$ m). This is intuitively attributed to the fact that the interference which is seen by the DMU from the MBSs is lower as their density λ_1 is smaller.

Fig. 3 shows the coverage probability of the DMU (see (14)). The coverage probability is plotted against N_d (the number of drones) and the drone altitude (h) in meters. As illustrated in Fig. 3, it can be observed that with an increase in the number of DBSs the optimal altitude is reduced for the DBSs. Thus, altitude control gives a new degree of freedom to the optimal deployment of the DSCN. Generally, the coverage probability values obtained with regard to the number of DBSs depends on two main factors: (i) the required total average network capacity, which intuitively increases as the number of DBSs increases and (ii) an increase in the number of channels deployed which translates into increases in the coverage probability.

Fig. 4(a) shows the coverage probability for DMU vs. the drone altitude for multiple network configurations (see (14)). Here, the solid lines correspond to the deployment geometry for a multiple number of drones for a disaster recovery area of radius $R_r = 2$ km while the dashed lines are for $R_r = 3$ km. The figure shows that the optimal drone altitude decreases as the number of drones increases. In turn, this corresponds to the decrease in interference experienced at the DMU. Also, an interesting observation is that a wider recovery area radius requires a higher drone altitude to maintain the same baseline coverage. Nevertheless, deploying DBSs at higher altitudes means that a smaller number of BSs are required to cover a wide recovery area. While this corresponds to a reduction in co-channel interference experienced at the DMU, this comes at the cost of reduced throughput. The down-link throughput of a MU increases with an increase in the number of DBSs due to aggregate load reduction on individual BSs.

Fig. 4(b) shows the coverage probability vs. drones altitude for the DMU for both: (i) the configurations when only DBSs are deployed (depicted with solid orange lines derived from (10)) and (ii) the configuration when the DBSs are overlaid on the operational cellular network (the dashed blue lines obtained from (14)). Here, we can observe two main trends: (i) good coverage can be achieved for the network deployment with only DBSs, and this can also be seen as allocating unique channels for the DBCN and (ii) there is a substantial need to search for the optimal altitude for the DBS, since the coverage probability dramatically decreases when an operational altitude other



(a) Coverage probability with both the DBSs and MBSs (see (14)).
(b) Coverage probability both the DBSs and MBSs (see (10) and (14)).
(c) Coverage probability of MMU with both the DBSs and MBSs(see (15)).

Fig. 4: Coverage Probability with $N_c = 3$, $p^o = 0.5$, $\lambda_1 = 1 \times 10^{-5}$, $\alpha = 4$, $R_r = 2 \text{ km}$ and $\beta = -3 \text{ dB}$

than the optimal altitude is selected.

Fig. 4(c) shows the coverage probability of MMU vs. the drone altitude for multiple network configurations (see (15)). The dashed green line shows the maximum achievable coverage of the MMU without the existence of the DSCN. Intuitively, this upper limit cannot be achieved in the presence of the DBSs, mainly due to non-zero co-channel interference which will be generated from the DBSs. For a recovery area with radius $R_r = 2 \text{ km}$, the optimal drone altitude is lower than $h = 600 \text{ m}$ (see Fig. 4(a)). Consequently, for $N_d = 9$ DBSs the optimal network altitude is around 500 m, while the coverage probability for the MMU with the same deployment configuration of the DBCN is around 0.75 (i.e., this means that the ratio $((P_c^{(m)} - \text{Maximum Coverage})/\text{Maximum Coverage}) \times 100 = 90\%$) which is quite acceptable with the advantage of a higher achieved $P_c^{(d)}$. Consequently, a DSCN can be deployed by only optimizing the number of drones and their altitude.

V. CONCLUSION

Drone empowered small cellular networks (DSCNs) are key enablers towards the deployment of resilient communication networks for smart cities. In this paper, we developed a statistical framework for exploring the design space of a DSCN under realistic propagation conditions. The impact of co-channel inter and intra-network interference, when a DSCN is deployed to complement a capacity short-fall in disaster recovery scenario, has explicitly accommodated in the model. In other words, the co-existence properties of overlaid DSCN networks are investigated. It is also shown that by optimizing the altitude of drone base stations (DBSs) and number of drones the coverage probability of a ground user can be significantly enhanced in a post-disaster situation. Moreover, this can be accomplished at a minimum loss of performance incurred at a micro mobile user (MMU) that being served by an operational ground cellular network. Overall, coverage probability of ground users is significantly enhanced when DSCN is deployed and the network design is appropriately optimized.

REFERENCES

- [1] I. Bucaille, S. Hethuin, T. Rasheed, A. Munari, R. Hermenier, and S. Allsopp, “Rapidly deployable network for tactical applications: Aerial base station with opportunistic links for unattended and temporary events absolute example,” in *Military Communications Conference, MILCOM IEEE*, pp. 1116–1120, 2013.
- [2] W. Guo, C. Devine, and S. Wang, “Performance analysis of micro unmanned airborne communication relays for cellular networks,” in *Communication Systems, Networks & Digital Signal 9th International Symposium on Processing (CSNDSP)*, pp. 658–663, IEEE, 2014.
- [3] M. Gharibi, R. Boutaba, and S. L. Waslander, “Internet of drones,” *arXiv preprint arXiv:1601.01289*, 2016.
- [4] M. Mozaffari, W. Saad, M. Bennis, and M. Debbah, “Drone small cells in the clouds: Design, deployment and performance analysis,” *arXiv preprint arXiv:1509.01655*, 2015.
- [5] X. Lin, J. Andrews, A. Ghosh, and R. Ratasuk, “An overview of 3gpp device-to-device proximity services,” *Communications Magazine, IEEE*, vol. 52, no. 4, pp. 40–48, 2014.
- [6] G. Baldini, S. Karanasiou, D. Allen, and F. Vergari, “Survey of wireless communication technologies for public safety,” *Communications Surveys & Tutorials, IEEE*, vol. 16, no. 2, pp. 619–641, 2014.
- [7] R. Ferrus, O. Sallent, G. Baldini, and L. Goratti, “Lte: the technology driver for future public safety communications,” *Communications Magazine, IEEE*, vol. 51, no. 10, pp. 154–161, 2013.
- [8] R. Yaliniz, A. El-Keyi, and H. Yanikomeroglu, “Efficient 3-d placement of an aerial base station in next generation cellular networks,” *arXiv preprint arXiv:1603.00300*, 2016.
- [9] A. Al-Hourani, S. Kandeepan, and S. Lardner, “Optimal lap altitude for maximum coverage,” *Wireless Communications Letters, IEEE*, vol. 3, no. 6, pp. 569–572, 2014.
- [10] S. N. Chiu, D. Stoyan, W. S. Kendall, and J. Mecke, *Stochastic geometry and its applications*. John Wiley & Sons, 2013.
- [11] S. Srinivasa and M. Haenggi, “Modeling interference in finite uniformly random networks,” in *International Workshop on Information Theory for Sensor Networks (WITS07)*, pp. 1–12, 2007.
- [12] 3GPP, “Further advancements for e-utra physical layer aspects,” tech. rep., 3GPP TR 36.814, 2010.
- [13] 3GPP, “Digital cellular telecommunications system (phase 2+); radio network planning aspects,” tech. rep., 3GPP TR 43.030, 2010.
- [14] H. Inaltekin, M. Chiang, H. V. Poor, and S. B. Wicker, “On unbounded path-loss models: effects of singularity on wireless network performance,” *Selected Areas in Communications, IEEE Journal on*, vol. 27, no. 7, pp. 1078–1092, 2009.
- [15] O. Georgiou, S. Wang, M. Z. Bocus, C. P. Dettmann, and J. P. Coon, “Location, location, location: Border effects in interference limited ad hoc networks,” in *13th International Symposium on Modeling and Optimization in Mobile, Ad Hoc, and Wireless Networks (WiOpt)*, pp. 568–575, IEEE, 2015.
- [16] S. A. R. Zaidi, D. C. McLernon, and M. Ghogho, “Breaking the area spectral efficiency wall in cognitive underlay networks,” *Selected Areas in Communications, IEEE Journal on*, vol. 32, no. 11, pp. 2205–2221, 2014.
- [17] M. Haenggi and R. K. Ganti, *Interference in large wireless networks*. Now Publishers Inc, 2009.
- [18] A. Jeffrey and D. Zwillinger, *Table of integrals, series, and products*. Academic Press, 2007.
- [19] S. Srinivasa and M. Haenggi, “Distance distributions in finite uniformly random networks: Theory and applications,” *IEEE Transactions on Vehicular Technology*, vol. 59, no. 2, pp. 940–949, 2010.